

M2 Macrophage-Derived Exosomal lncRNA AFAP1-AS1 and MicroRNA-26a Affect Cell Migration and Metastasis in Esophageal Cancer

Xifeng Mi,¹ Rongyu Xu,² Shunzhong Hong,¹ Tingting Xu,¹ Wanfei Zhang,² and Ming Liu³

¹Department of Gastroenterology, Quanzhou First Hospital Affiliated to Fujian Medical University, Quanzhou, 362000 Fujian, China; ²Department of Oncology, Quanzhou First Hospital Affiliated to Fujian Medical University, Quanzhou, 362000 Fujian, China; ³Digestive Endoscopy Center of the First Affiliated Hospital of Xiamen University, Xiamen, 361000 Fujian, China

Exosomes from cancer cells or immune cells, carrying biomacromolecules or long non-coding RNAs (lncRNAs), participate in tumor pathogenesis and progression by modulating the microenvironment. This study aims to explore the function of M2 macrophage-derived exosomes on the invasion and metastasis of esophageal cancer (EC) with the involvement of the lncRNA AFAP1-AS1/microRNA-26a (miR-26a)/activating transcription factor 2 (ATF2) axis. We found that lncRNA AFAP1-AS1 could specifically bind to miR-26a, thus affecting the expression of miR-26a, and ATF2 was the direct target of miR-26a. Compared with M1 macrophage-derived exosomes, M2 macrophage-derived exosomes exhibited higher AFAP1-AS1 and ATF2 expression and lower miR-26a expression. Moreover, extracellular AFAP1-AS1 could be moved to KYSE410 cells via being incorporated into M2 macrophage-derived exosomes. M2 macrophage-derived exosomes could downregulate miR-26a and promote the expression of ATF2 through high expression of AFAP1-AS1, thus promoting the migration, invasion, and lung metastasis of EC cells; M2-exosomes upregulating AFAP1-AS1 or downregulating miR-26a ameliorated this effect. In summary, M2 macrophage-derived exosomes transferred lncRNA AFAP1-AS1 to downregulate miR-26a and upregulate ATF2, thus promoting the invasion and metastasis of EC. Targeting M2 macrophages and the lncRNA AFAP1-AS1/miR-26a/ATF2 signaling axis represents a potential therapeutic strategy for EC.

INTRODUCTION

Esophageal cancer (EC) ranks eighth in most common cancers worldwide and sixth in cancer mortality, and it mainly includes squamous cell carcinoma and adenocarcinoma.^{1,2} It has been reported that China is a country with very high EC incidence, and the Taihang Mountains region is the highest in the world, where carcinogen exposure and malnutrition account for the chief risk factors for EC, instead of cigarettes and alcohol.³ Common cancer therapies including surgery, radiation, and chemotherapy are current treatments for EC, and tumor markers of EC are expected to contribute to earlier diagnosis of this disease.³ In recent years, macrophages have been pro-

posed to affect cancer development and patients' prognosis,⁴ as a result of which we are inspired to find new treatment of EC from M2 macrophage-derived exosomes.

Exosomes are membrane vesicles derived from diverse cells with a diameter of 40 to 100 nm, which contain many substances such as nucleic acids, proteins, and enzymes.⁵ The contributory effects of exosomes on tumor progression have been discovered.⁶ Evidence has shown that exosomes derived from T cells may boost the epithelial-to-mesenchymal transition (EMT) in EC cells by upregulating β -catenin and nuclear factor κ B (NF- κ B)/snail pathway, thus contributing to EC metastasis.⁷ Actin filament associated protein 1 antisense RNA1 (AFAP1-AS1), one long non-coding RNA (lncRNA), has also been reported to be abnormally expressed in some cancers and correlated with cancer development.^{8,9} AFAP1-AS1 has been suggested to be overexpressed in esophageal squamous cell carcinoma (ESCC), thus boosting its cell proliferation and restricting its apoptosis.¹⁰ Yuan et al.¹¹ have demonstrated that AFAP1-AS1 is capable of targeting microRNA (miRNA)-320a (miR-320a) to affect cell stemness and chemoresistance of laryngeal carcinoma. It has been indicated that microRNA-26a (miR-26a) is a tumor inhibitor in a variety of cancers.¹² Li et al.¹³ have revealed that ESCC growth can be circumscribed by miR-26a and miR-26b. A study has shown that activating transcription factor 2 (ATF2) is directly targeted by miR-26a.¹⁴ There has been a study indicating that ATF2 is in close relation to ESCC patients' comprehensive survival.¹⁵ Nevertheless, the role of M2 macrophage-derived exosomes in EC remains obscure. Therefore, this study aims to explore the mechanism of lncRNA AFAP1-AS1 derived from M2 macrophage exosomes on EC invasion and metastasis via modulating the miR-26a/ATF2 pathway.

Received 27 May 2020; accepted 30 September 2020;
<https://doi.org/10.1016/j.omtn.2020.09.035>.

Correspondence: Xifeng Mi, PhD, Department of Gastroenterology, Quanzhou First Hospital Affiliated to Fujian Medical University, No. 250, Dongjie Street, Licheng District, Quanzhou, 362000 Fujian, China.
E-mail: mixifeng2089@163.com



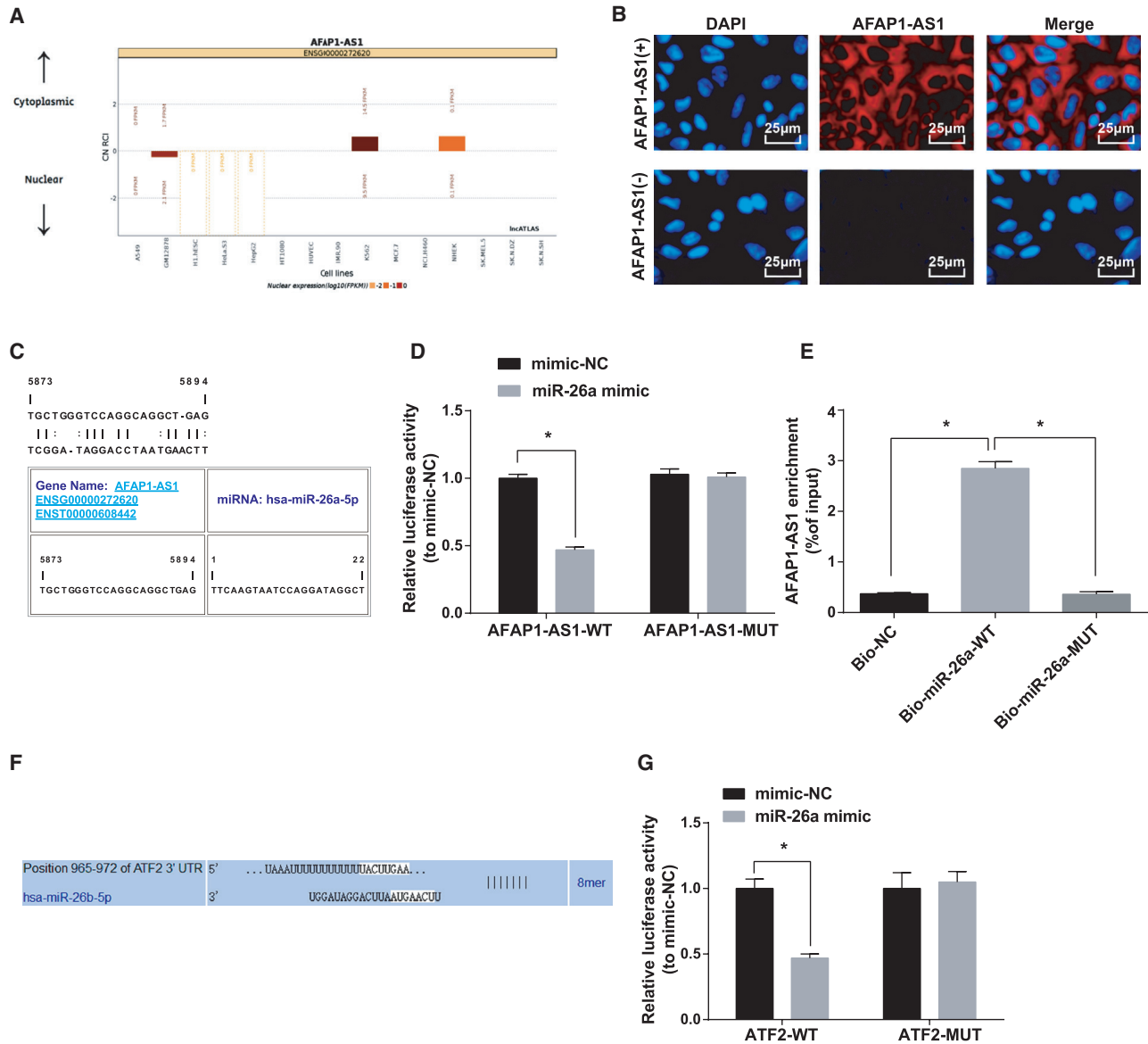


Figure 1. ATF2 Is a Direct Target Gene of miR-26a and AFAP1-AS1 Absorbs miR-26a to Impact Its Expression

(A) Prediction of AFAP1-AS1 subcellular localization by online analysis site. (B) Verification of AFAP1-AS1 subcellular localization by FISH assay (400 \times ; scale bars, 25 μ m). (C) Prediction of the binding site of AFAP1-AS1 and miR-26a by RNA22 site. (D) Verification of AFAP1-AS1 binding to miR-26a by dual luciferase reporter gene assay. (E) Detection of miR-26a's enrichment of AFAP1-AS1 by RNA pull-down assay. (F) Prediction of the targeting site between miR-26a and ATF2 by TargetsCan website. (G) Verification of the targeting site between miR-26a and ATF2 by dual luciferase reporter gene assay. * $p < 0.05$. $N = 3$. The data in the figure were all measurement data expressed as mean \pm standard deviation; the t test was used for comparison between two groups, and ANOVA was used for the comparison among multiple groups, after which pairwise comparison was made by Tukey's multiple comparisons test.

RESULTS

ATF2 Is a Direct Target Gene of miR-26a, and AFAP1-AS1 Sponges miR-26a to Impact Its Expression

Previous studies have shown that some specific lncRNAs may operate as competing endogenous RNAs (ceRNAs) in carcinogenesis. ceRNAs can function as miRNA sponges to modulate miRNAs, which functionally liberates mRNA transcripts targeted by miRNAs.^{16,17}

To clarify the functional mechanisms of AFAP1-AS1, we first analyzed AFAP1-AS1 online at <http://lncatlas.org/eu/> to explore its mechanism. The results showed that AFAP1-AS1 was mainly distributed in the cytoplasm (Figure 1A), which was further verified by RNA fluorescence *in situ* hybridization (FISH) assay, indicating that AFAP1-AS1 may function in the cytoplasm (Figure 1B). Through the RNA22 website (<https://cm.jefferson.edu/rna22/Precomputed/>),

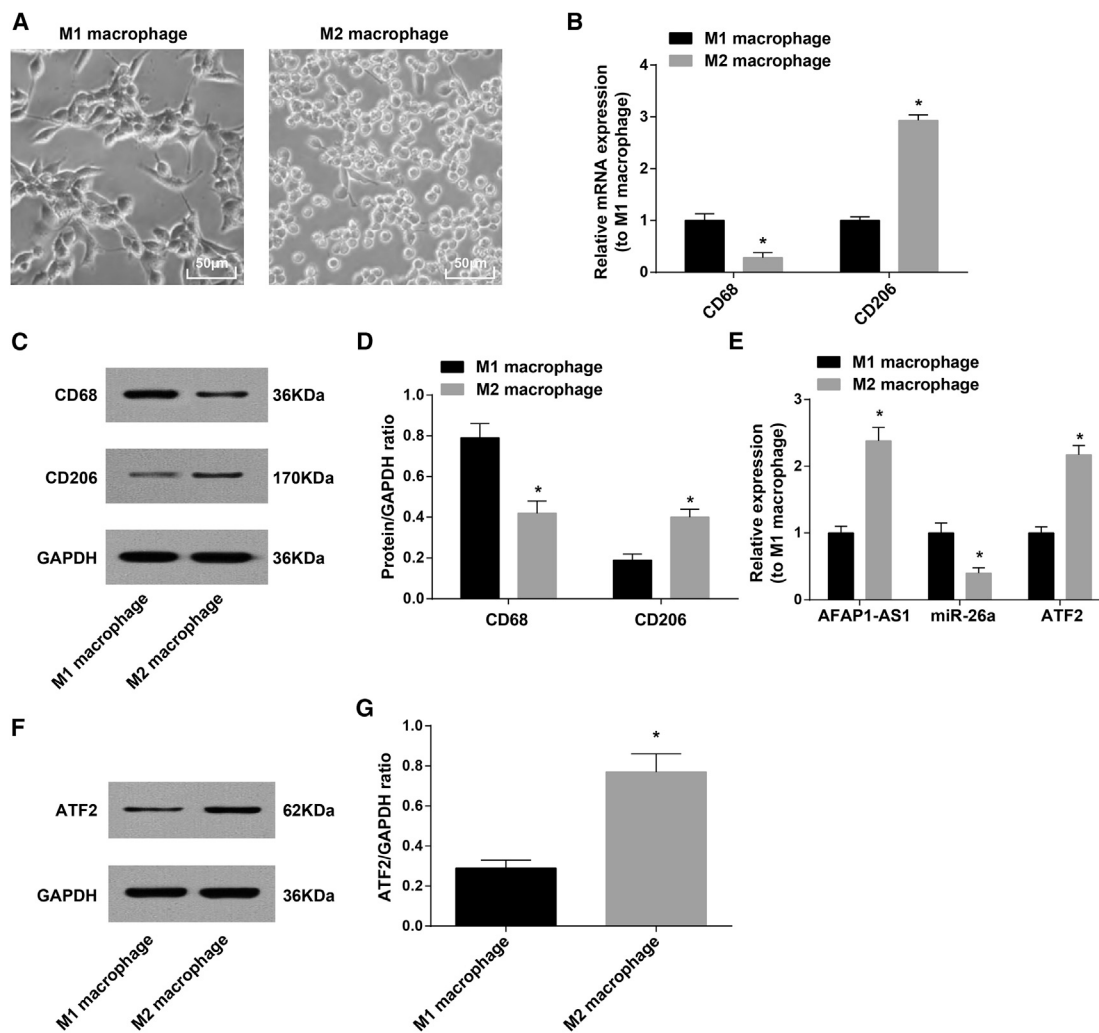


Figure 2. Identification of M2 Macrophages

(A) Morphology of M1 and M2 macrophages was observed under an inverted microscope (400 \times , scale bars, 50 μ m). (B) CD68 and CD206 mRNA expression in M1 and M2 macrophages detected by qRT-PCR. (C) Protein bands of CD68 and CD206 in M1 and M2 macrophages. (D) CD68 and CD206 protein expression in M1 and M2 macrophages detected by western blot analysis. (E) AFAP1-AS1, miR-26a, and ATF2 mRNA expression in M1 and M2 macrophages detected by qRT-PCR. (F) Protein band of ATF2 in M1 and M2 macrophages. (G) ATF2 protein expression in M1 and M2 macrophages detected by western blot analysis. * $p < 0.05$ versus M1 macrophages. $N = 3$. The data were expressed as mean \pm standard deviation and analyzed by t test.

it was found that AFAP1-AS1 could bind to miR-26a (Figure 1C). Subsequent verification by dual luciferase reporter gene assay revealed that the luciferase activity of cells co-transfected with AFAP1-AS1-wild-type (WT) and miR-26a mimic was reduced a lot ($p < 0.05$), while no big difference was seen in the activity of cells co-transfected with AFAP1-AS1-mutant (MUT) and miR-26a mimic ($p > 0.05$), showing that miR-26a may specifically bind to AFAP1-AS1 (Figure 1D). RNA pull-down assay was adopted to verify that AFAP1-AS1 could be a ceRNA to absorbing miR-26a. The results indicated that AFAP1-AS1 enrichment elevated greatly in the biotin-labeled (Bio)-miR-26a-WT group versus the Bio-negative control (NC) group ($p < 0.05$), yet no clear difference in the enrichment was seen in the Bio-miR-26a-MUT group ($p > 0.05$; Figure 1E). These

results indicated that lncRNA AFAP1-AS1 could sponge miR-26a, thereby impacting its expression.

We found that the binding sites of miR-26a matched the 3' untranslated region (UTR) of ATF2 according to Targetscan (http://www.targetscan.org/vert_72/) (Figure 1F). This suggests that ATF2 is a potential target of miR-26a. Results from a dual luciferase reporter gene assay showed that the luciferase activity of KYSE410 cells declined obviously after ATF2-WT and miR-26a mimic co-transfection ($p < 0.05$), while no changes were found in the luciferase activity after ATF2-MUT and miR-26a mimic co-transfection ($p > 0.05$), indicating that ATF2 is a direct target gene of miR-26a (Figure 1G).

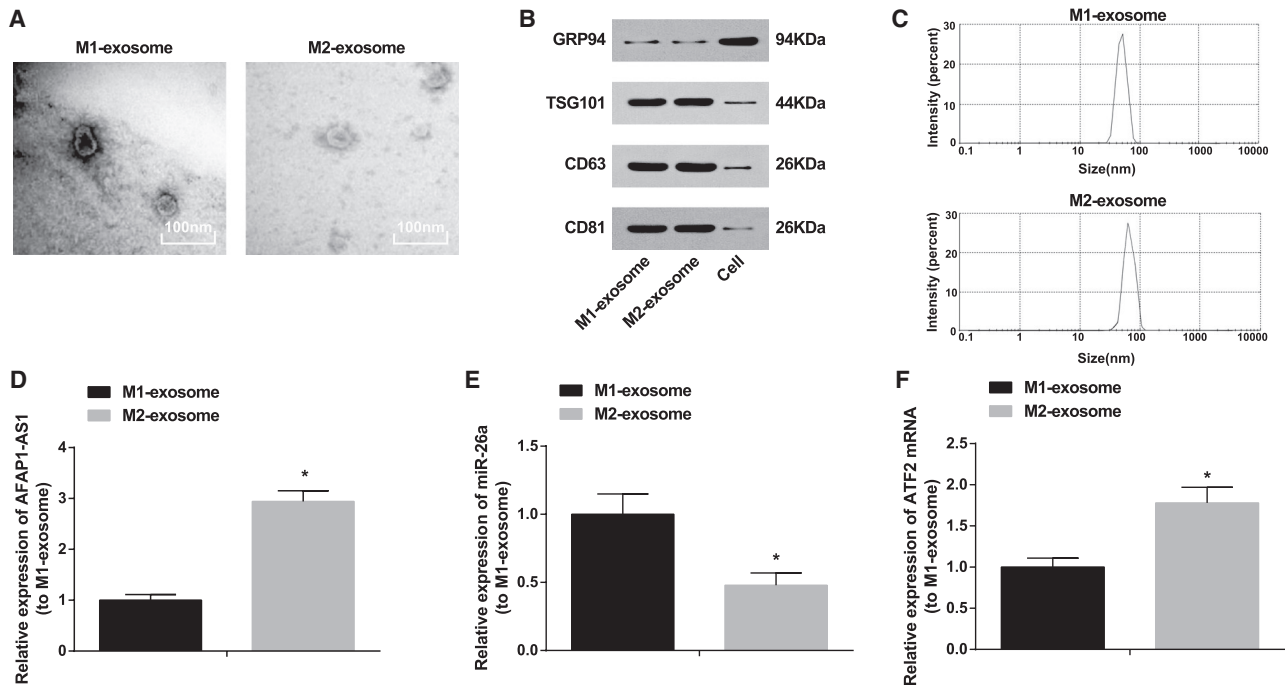


Figure 3. AFAP1-AS1 and ATF2 Expression Is Upregulated and miR-26a Is Downregulated in M2 Macrophage-Derived Exosomes

(A) Exosome morphology observation under TEM (20,000 \times ; scale bars, 100 nm). (B) Protein bands of CD63, CD81, TSG101, and GRP94 in M1 and M2 exosomes. (C) Nanoparticle tracing analysis of size distribution of exosomes. (D) AFAP1-AS1 expression in M1 and M2 exosomes detected by qRT-PCR. (E) miR-26a expression in M1 and M2 exosomes detected by qRT-PCR. (F) ATF2 mRNA expression in M1 and M2 exosomes detected by qRT-PCR. * $p < 0.05$ versus M1 exosome. $N = 3$. The data were expressed as mean \pm standard deviation and analyzed by independent sample t test.

Identification of M2 Macrophages

We separately stimulated human peripheral blood mononuclear cells (PBMC) with granulocyte-macrophage colony-stimulating factor (GM-CSF) and macrophage colony-stimulating factor (M-CSF). Treatment with GM-CSF induced the M1 phenotype and the shape was mainly round, whereas M-CSF-activated M2 phenotype was in spindle (Figure 2A).

CD68 and CD206 expression was detected by quantitative reverse transcriptase polymerase chain reaction (qRT-PCR) and western blot analysis to identify M1 and M2 macrophages. The results showed a marked decrease in CD68 expression in M2 macrophages and a palpable growth in CD206 expression versus in M1 macrophages ($p < 0.05$; Figures 2B–2D). AFAP1-AS1, miR-26a, and ATF2 expression in macrophages was also detected by qRT-PCR and western blot analysis. The results indicated upregulated AFAP1-AS1 and ATF2 expression and downregulated miR-26a in M2 macrophages versus M1 macrophages ($p < 0.05$; Figures 2E–2G).

AFAP1-AS1 and ATF2 Expression Is Upregulated and miR-26a Is Downregulated in M2 Macrophage-Derived Exosomes

Transmission electron microscopy (TEM) results showed the morphology of M1-exosome and M2-exosome as round or round-like vesicles with a diameter of 30–100 nm and a bilayer lipid mem-

brane. The surrounding area was densely stained, with clear edges versus the central area, and distinctive manifestations of exosomes were observed (Figure 3A). Western blot analysis showed that, M1-exosome and M2-exosome expressed exosome marker proteins CD63, CD81, and TSG101 yet nearly did not express GRP94 protein (Figure 3B). Nanoparticle tracking analysis (NTA) results indicated that the exosome diameter mainly distributed at 30–100 nm (Figure 3C). qRT-PCR showed that, versus M1-exosome, AFAP1-AS1 and ATF2 were overexpressed, while miR-26a was downregulated in M2-exosome ($p < 0.05$; Figures 3D–3F).

M2-Exosome Promotes Cell Migration and Invasion as well as *In Vitro* Lung Tumor Metastasis in EC

Studies have indicated that M2 macrophages or M2-exosomes promoted the progression of pancreatic and gastric cancers.^{18–21} However, the role of M2 macrophages in EC development remains largely unknown. Thus, we investigated the effect of M2 macrophages on malignant phenotypes of EC cells. It has been reported that macrophages can promote EC metastasis by secreting some factors; hence, we studied whether M2-exosomes have impact on the biological functions of EC cells.

Uptake assay showed that there appeared red fluorescence-labeled M2-exosome around the KYSE410 cells (4',6-diamidino-2-phenylindole, dihydrochloride [DAPI]) after the cells were co-incubated with

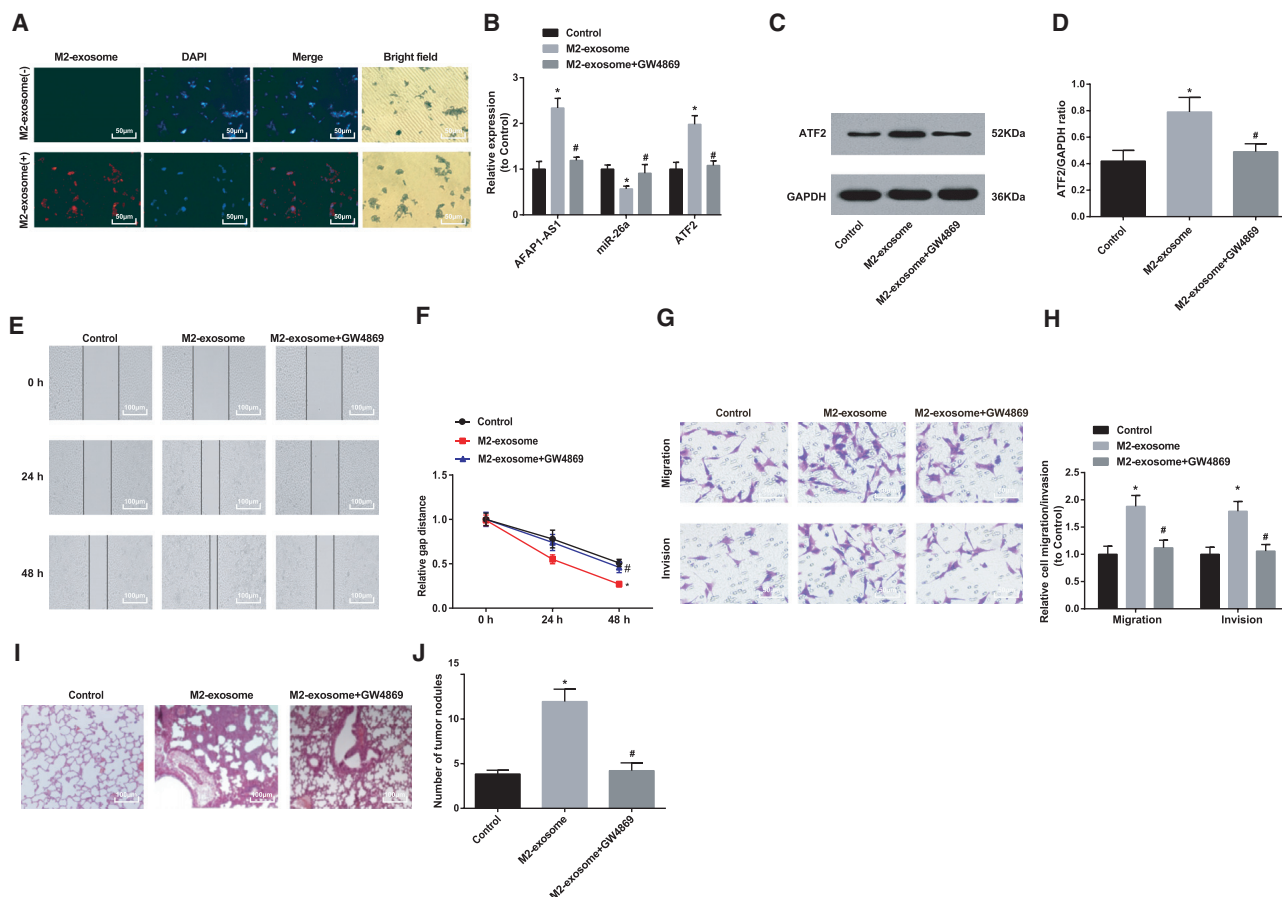


Figure 4. M2-Exosome Promotes Cell Migration and Invasion as well as *In Vitro* Lung Tumor Metastasis in EC

(A) Observation of uptake of M2-exosome by KYSE410 cells using confocal microscopy (400 \times ; scale bars, 50 μ m). (B) Expression of AFAP1-AS1, miR-26a, and ATF2 in KYSE410 cells after co-culture with M2 macrophages. (C) Protein band of ATF2 in KYSE410 cells after co-culture with M2 macrophages. (D) Protein expression of ATF2 in KYSE410 cells after co-culture with M2 macrophages. (E) Wound healing distance in the control and M2-exosome groups. (F) Effect of M2-exosome on wound healing distance of KYSE410 cells. (G) Representative figure for cell migration and invasion by Transwell assay. (H) Effects of M2-exosome on the number of migration and invasion KYSE410 cells. (I) Observation of lung metastasis in nude mice tumor tissue by H&E staining (200 \times ; scale bars, 100 μ m). (J) Number of lung metastasis nodules in the control and M2-exosome groups. * $p < 0.05$ versus control group; # $p < 0.05$ versus M2-exosome group. $N = 3$. The data are expressed as mean \pm standard deviation, and ANOVA was used for the comparison among multiple groups, after which pairwise comparison was made by Tukey's multiple comparisons test.

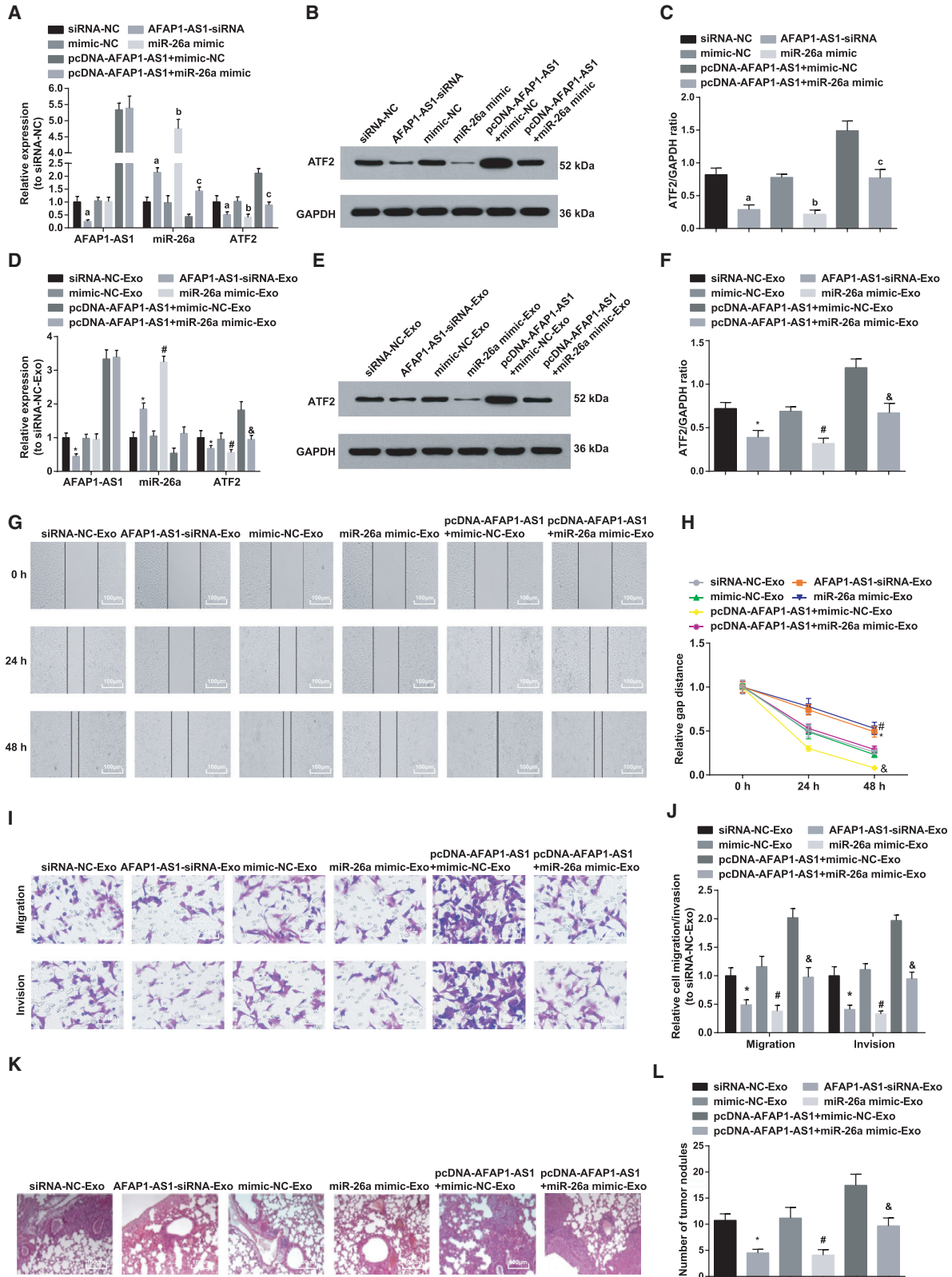
Dil-labeled M2-exosome, while the red fluorescence was not found in the NC group (Figure 4A).

Results of qRT-PCR and western blot analysis reflected that cells in the M2-exosome group had increased AFAP1-AS1 and ATF2 expression and decreased miR-26a expression versus the control group (all $ps < 0.05$); treatment of GW4869 reduced AFAP1-AS1 and ATF2 expression and promoted miR-26a expression in KYSE410 cells (all $ps < 0.05$); expression of AFAP1-AS1, miR-26a, and ATF2 showed no significant difference in cells between the control and M2-exosome + GW4869 groups (all $ps > 0.05$; Figures 4B–4D).

A scratch test revealed that cell migration distance after 24- and 48-h scratching in the M2-exosome group was noticeably longer than that in the control group; treatment of GW4869 suppressed the

migration distance ($p < 0.05$); no difference in cell migration distance could be found between the control and M2-exosome + GW4869 groups ($p > 0.05$; Figures 4E and 4F). Transwell migration and invasion assay indicated higher migration and invasion ability in the M2-exosome group than in the control group; while migration and invasion ability were inhibited by GW4869 ($p < 0.05$), no evident difference in migration and invasion ability was found between the control and M2-exosome + GW4869 groups ($p > 0.05$; Figures 4G and 4H).

Hematoxylin and eosin (H&E) staining showed that the lung tissue in the control and M2-exosome + GW4869 groups gradually grew like a nest, and the tumor cells were arranged closely and orderly. However, the lung metastasis focus of the nude mice in the M2-exosome group rose substantially relative to the control group ($p < 0.05$), and the



(legend on next page)

tumor cells were diffusely distributed with large size, deeply stained nuclei, and obvious nucleoli (Figures 4I–4J).

M2-Exosomes Upregulate miR-26a or Downregulate AFAP1-AS1 to Reverse the Contributory Impacts of M2-Exosomes on Cell Migration and Invasion as well as *In Vitro* Lung Tumor Metastasis in EC

The aforementioned results revealed that AFAP1-AS1 was differentially expressed when M2-exosomes acted on EC cells. To identify the impact of M2-exosomes transferring AFAP1-AS1 on invasion and migration of EC cells, we established co-culture models to explore the role of M2-exosomes shuttling in EC cells. M2 macrophages transfected with silenced AFAP1-AS1 plasmid, overexpressed AFAP1-AS1 plasmid, or miR-26a mimic were co-cultured with EC cells to detect their effect on the migration and invasion ability of EC cells. The lung metastasis of EC in a mouse model was performed to assess the role of M2-exosomes on EC cell migration *in vivo*. qRT-PCR and western blot analysis were used to assess expression of AFAP1-AS1, miR-26a, and ATF2 in M2 macrophages after relative transfection (oligonucleotides or plasmids related to AFAP1-AS1 or miR-26a). The results showed that AFAP1-AS1 and ATF2 expression in the AFAP1-AS1-small interfering RNA (siRNA) group dropped a lot versus that in the siRNA-NC group, while miR-26a expression grew markedly (all p s < 0.05). Compared with expression in the mimic-NC group, ATF2 expression in the miR-26a mimic group diminished noticeably, which was contrary to the difference in miR-26a expression (both p s < 0.05), and AFAP1-AS1 expression was hardly changed (p > 0.05). We further explored the reversal effect of miR-26a on the impacts of AFAP1-AS1 overexpression on AFAP1-AS1, miR-26a, and ATF2 expression in KYSE410 cells and found that, versus the pcDNA-AFAP1-AS1 + mimic-NC group, ATF2 expression in the pcDNA-AFAP1-AS1 + miR-26a mimic group fell dramatically, while miR-26a expression showed an opposite trend (both p s < 0.05), and AFAP1-AS1 expression was not markedly changed (p > 0.05; Figures 5A–5C).

AFAP1-AS1, ATF2, and miR-26a expression in KYSE410 receptor cells after co-culture with M2 macrophages after relative transfection (oligonucleotides or plasmids related to AFAP1-AS1 or miR-26a) was determined using qRT-PCR and western blot analysis. It was found that the AFAP1-AS1-siRNA-Exosome (Exo) group had decreased AFAP1-AS1 and ATF2 expression and increased miR-26a expression versus the siRNA-NC-Exo group (p < 0.05); in relation to the mimic-

NC-Exo group, ATF2 expression was reduced, miR-26a expression was enhanced (both p s < 0.05), and AFAP1-AS1 expression was not altered (p > 0.05) in the miR-26a mimic-Exo group. Versus the pcDNA-AFAP1-AS1 + mimic-NC-Exo group, ATF2 expression was decreased, miR-26a expression was elevated (both p s < 0.05) and AFAP1-AS1 did not change (p > 0.05) in the pcDNA-AFAP1-AS1 + miR-26a mimic-Exo group (Figures 5D–5F).

After co-culture of all M2 macrophages that had been transfected with oligonucleotides or plasmids related to AFAP1-AS1 or miR-26a with EC KYSE410 cells, the scratch test was applied for detecting the effect of M2 macrophage-derived exosomal lncRNA AFAP1-AS1 and miR-26a on KYSE410 cell migration. The results showed that, after 24- and 48-h scratching, the cell migration distance in the AFAP1-AS1-siRNA-Exo group was far shorter than that of the siRNA-NC-Exo group (p < 0.05); the same parameter in the miR-26a mimic-Exo group was greatly shortened (p < 0.05) versus that in the mimic-NC-Exo group. We further observed the reversal effect of miR-26a on the impacts of AFAP1-AS1 overexpression on KYSE410 cell migration distance in co-culture system and found that the cell migration distance in the pcDNA-AFAP1-AS1 + miR-26a mimic-Exo group decreased noticeably versus that in the pcDNA-AFAP1-AS1 + mimic-NC-Exo group (p < 0.05; Figures 5G and 5H).

After co-culture of all M2 macrophages that had been transfected with oligonucleotides or plasmids related to AFAP1-AS1 or miR-26a with KYSE410 cells, Transwell assay was adopted for the determination of the effect of M2 macrophage-derived exosomal lncRNA AFAP1-AS1 and miR-26a on KYSE410 cell migration and invasion. It was found that the invasion and migration ability in the AFAP1-AS1-siRNA-Exo group reduced palpably versus that in the siRNA-NC-Exo group (p < 0.05). Compared with that in the mimic-NC-Exo group, the same parameter in the miR-26a mimic-Exo group dropped clearly (p < 0.05). We further observed the reversal effect of miR-26a on the impacts of AFAP1-AS1 overexpression on KYSE410 cell invasion and migration in co-culture system and found that cell invasion and migration ability in the pcDNA-AFAP1-AS1 + miR-26a mimic-Exo group fell substantially versus that in the pcDNA-AFAP1-AS1 + mimic-NC-Exo group (p < 0.05; Figures 5I and 5J).

H&E staining showed that, compared with the siRNA-NC-Exo group, the AFAP1-AS1-siRNA-Exo group showed a clear reduction in lung

Figure 5. M2-Exosomes Upregulate miR-26a or Downregulate AFAP1-AS1 to Reverse the Contributory Impacts of M2-Exosomes on Cell Migration and Invasion, as well as *In Vitro* Lung Tumor Metastasis in EC

(A) AFAP1-AS1, miR-26a, and ATF2 mRNA expression in M2 macrophages of each group detected by qRT-PCR. (B) Protein band of ATF2 in M2 macrophages in each group. (C) ATF2 protein expression in M2 macrophages in each group detected by western blot analysis. (D) AFAP1-AS1, miR-26a, and ATF2 mRNA expression in KYSE410 cells of each group detected by qRT-PCR. (E) Protein band of ATF2 in KYSE410 cells of each group. (F) Protein expression of ATF2 in KYSE410 cells of each group. (G) Representative figure for cell migration by scratch test. (H) Wound healing distance in each group. (I) Representative figure for cell migration and invasion by Transwell assay. (J) Effects of lncRNA AFAP1-AS1 and miR-26a on the migration and invasion of KYSE410 cells. (K) Observation of lung metastasis in nude mice by H&E staining (100 \times ; scale bars, 100 μ m). (L) Number of lung metastases in each group. ^a p < 0.05 versus the siRNA-NC group; ^b p < 0.05 versus the mimic-NC group; ^c p < 0.05 versus the pcDNA-AFAP1-AS1 + mimic-NC group; ^d p < 0.05 versus the siRNA-NC-Exo group; ^e p < 0.05 versus the mimic-NC-Exo group; ^f p < 0.05 versus the pcDNA-AFAP1-AS1 + mimic-NC-Exo group. $N = 3$. The data are expressed as mean \pm standard deviation, and ANOVA was used for the comparison among multiple groups, after which pairwise comparison was made by Tukey's multiple comparisons test.

tissue metastasis focus ($p < 0.05$), closely and orderly arranged tumor cells that were diffusely distributed, and not so deeply stained nuclei; compared with the mimic-NC-Exo group, the miR-26a mimic-Exo group indicated a similar result as described earlier ($p < 0.05$). Then we further examined the reversal effect of miR-26a on the impacts of AFAP1-AS1 overexpression on lung metastasis in tumor tissues and discovered that, in the pcDNA-AFAP1-AS1 + miR-26a mimic-Exo group, lung metastasis focus decreased substantially (both $ps < 0.05$), and closely and orderly arranged cells along with alleviated diffuse distribution of tumor cells and nuclear staining were observed relative to the pcDNA-AFAP1-AS1 + mimic-NC-Exo group (Figures 5K and 5L).

DISCUSSION

ES is a non-negligible disease with an extremely high morbidity and mortality.²² Nowadays, salvage esophagectomy is deemed as the only therapy likely to supply long-term survival for EC patients receiving definitive chemoradiotherapy, yet high morbidity and mortality are still ineluctable.²³ Recently, associations between M2 macrophages and gastric cancer development have been found.²¹ Nevertheless, the role of M2 macrophage-derived exosomes in EC remains to be examined. Thus, this study is intended for the exploration of the mechanism of M2 macrophage exosome-derived lncRNA AFAP1-AS1 on EC invasion and metastasis via modulating the miR-26a/ATF2 pathway. To conclude, our study revealed that M2 exosomes promoted the growth of EC cells and that upregulation of miR-26a reversed the contributory impacts of overexpressed AFAP1-AS1 in M2 macrophage-derived exosomes on cell migration and invasion as well as *in vitro* lung tumor metastasis in EC.

Based on the assays, our initial findings were that ATF2 was a direct target gene of miR-26a and that AFAP1-AS1 sponged miR-26a to impact its expression. In compliance with our study, a previous study has proved that ATF2 is a direct target gene of miR-26a.¹⁴ A similar study by Arora et al.²⁴ has also revealed that ATF2 is miR-26b's target gene. There has been a study showing that, in osteoarthritis (OA), lncRNA SNHG5 works as a sponge to competitively bind to miR-26a, thus functioning in OA development.²⁵ Tian et al.²⁶ have also demonstrated that lncRNA UCA1 modulates vascular smooth muscle cell progression by negatively targeting miR-26a. Another key finding of our study was that AFAP1-AS1 and ATF2 expression was upregulated and that miR-26a was downregulated in M2 macrophages and M2 macrophage-derived exosomes. It has been verified by Gezer et al.²⁷ that lncRNAs such as lncRNA TUG1 and lncRNA GAS5 are differently abundant in exosomes. An early report has shown that ATF2 is actively expressed in M1 macrophages in obese adipose tissue.²⁸ Also, reduction of miR-26a expression has been reported in mycobacterium tuberculosis-infected macrophages.²⁹

Moreover, we found that M2 macrophage-derived exosomes promoted cell migration and invasion as well as *in vitro* lung tumor metastasis in EC. In accordance with our study, an early study has illustrated that irradiated EC-infiltrating, T cell-derived exosomes

boost EC metastasis through EMT induction.⁷ It has been indicated that exosomes are capable of boosting the signal transduction between cancer cells and their recipient cells through the release of various biological molecules, thus influencing the communication of distant cancer cells in the tumor microenvironment with the progress of breast cancer.⁵ Further assays in our study suggested that upregulated miR-26a reversed the contributory impacts of overexpressed AFAP1-AS1 in M2 macrophage exosomes on cell migration and invasion of EC. Evidence has revealed that, in breast cancer, elevated miR-26b functions biologically in trastuzumab-induced cell growth restriction through the modulation of cyclin E2.³⁰ Also, there is a report showing that miR-26a and miR-26b exert negative effects on ESCC multiplication via restriction of c-MYC pathway.¹³ A study by Luo et al.¹⁰ has demonstrated that overexpressed AFAP1-AS1 in ESCC contributes to its cell proliferation and depresses apoptosis. Furthermore, upregulated AFAP1-AS1 in ESCC has been proposed to be in close relation to shorter progression-free survival and unfavorable overall survival.³¹

MATERIALS AND METHODS

Ethics Statement

Animals were treated humanely using approved procedures in compliance with the recommendations in the Guide for the Care and Use of Laboratory Animals of the National Institutes of Health. The protocol was approved by the Institutional Animal Care and Use Committee of Quanzhou First Hospital Affiliated to Fujian Medical University (ethical number: 201801013).

Cell Culture

Human peripheral blood mononuclear cells (PBMCs) supplied by Shanghai Huzhen Biotechnology (Shanghai, China), and KYSE410 cells supplied by Shanghai Meixuan Biological Science and Technology (Shanghai, China) were cultured in RPMI 1640 medium (GIBCO, Carlsbad, CA, USA) containing 10% fetal bovine serum (FBS) in an incubator (37°C, 5% CO₂, saturated humidity). When the cell confluence achieved 80% to 90%, the cells were detached with 0.25% trypsin before passage. The liquid was changed once every 2–3 days, and the cells in the logarithmic growth phase were taken for experiments.

Induction and Identification of M1 and M2 Macrophages

For the induction of M1 macrophages, human PBMCs were isolated for adherence overnight with the upper suspended cells removed and the adherent ones left. Then, PBMCs were stimulated by 800 U/mL GM-CSF (PeproTech, Rocky Hill, NJ, USA) for 7 days and cultured in a CO₂ cell-culture incubator at 37°C for differentiation into M1 macrophages. For the induction of M2 macrophages, after being treated as described earlier, the PBMCs were stimulated by 100 ng/mL M-CSF (PeproTech, Rocky Hill, NJ, USA) for 7 days to differentiate into M2 macrophages.

M1 and M2 macrophages were identified via detection of CD68 and CD206 expression by qRT-PCR and western blot analysis.

Table 1. Primer Sequence

Gene	Primer Sequence
miR-26a	forward: 5'-GGATCCGCAGAACTCCAGAGA-3' reverse: 5'-TTGGAGGAAAGACGATTTCGGT-3'
U6	forward: 5'-CTCGCTTCGGCAGCACATATACT-3' reverse: 5'-ACGCTTACGAATTTGCGTGTC-3'
AFAP1-AS1	forward: 5'-TCGCTCAATGGAGTGACGGCA-3' reverse: 5'-CGGCTGAGACCGCTGAGAAGCTT-3'
ATF2	forward: 5'-TGCCTGTTGCTATTCTGC-3' reverse: 5'-GCTCTTCTCCGACGACCACT-3'
CD68	forward: 5'-GCTACATGGCGGTGGAGTACAA-3' reverse: 5'-ATGATGAGAGGCAGCAAGATGG-3'
CD206	forward: 5'-TTCGGACACCCATCGGAATTT-3' reverse: 5'-CACAAAGCGCTGCGTGAT-3'
GAPDH	forward: 5'-ACGGCAAGTTCAACGGCACAG-3' reverse: 5'-GACGCCAGTAGACTCCACGACA-3'

miR-26a, microRNA-26a; ATF2, activating transcription factor 2; GAPDH, glyceraldehyde-3-phosphate dehydrogenase.

Extraction, Identification, and Labeling of Exosomes

For the extraction of exosomes: M1 and M2 macrophages in logarithmic growth phase were detached and routinely cultured for 48 h with exosome-free RPMI 1640 medium (GIBCO, Carlsbad, CA, USA) containing 10% FBS. The supernatant was collected; centrifuged at 4°C at $500 \times g$ for 10 min and $12,000 \times g$ for 20 min, respectively; and filtered through a 0.22- μm -pore filter, followed by centrifugation at ultra-high speed ($100,000 \times g$ for 2 h). Then, the precipitates were resuspended in phosphate-buffered saline (PBS) after the supernatant was removed and ultracentrifuged again for 2 h, followed by resuspension in PBS and storage at -80°C .

In the identification of exosomes: first, exosomes (30 μL) resuspended in $1 \times \text{PBS}$ were dropped on a copper mesh with a diameter of 2 mm and supplemented with 1% uranium acetate solution for 10-min negative staining, followed by drying with filter paper and air drying. Then, the copper mesh was placed under a transmission electron microscope (Hitachi High-Technologies, Tokyo, Japan) for morphology observation. Second, western blot analysis was used to identify the exosome surface markers. The exosome suspension was concentrated, and the protein content was determined by bicinchoninic acid (BCA) kits (23227, Thermo Fisher Scientific, Waltham, MA, USA). After sodium dodecyl sulfate-polyacrylamide gel electrophoresis and denaturation, the proteins were transferred onto membranes, and expression of exosome-specific marker proteins CD63, CD81, tumor susceptibility gene 101 (TSG101), and GRP94 was assessed. Third, Nanoparticle tracking

analysis (NTA) was used to analyse the extracted exosome using the Nano-Sight LM10 (Malvern Instruments, Inc., Malvern, UK). Diluted exosome samples performed Brownian movement for 60 s, and then the concentration and size distribution of the nanoparticles were calculated.

For detection of the uptake of M2 exosomes by KYSE410 cells by fluorescent labeling: M2-exosomes were obtained through resuspension in 500 μL $1 \times \text{PBS}$ in 1.5 mL Eppendorf (EP) tubes. The exosomes were stained with Dil dye solution (Beyotime, Shanghai, China) for 20 min with light avoidance, and the redundant dye solution was removed using an exosome staining filter column (Thermo Fisher Scientific). The treated exosomes were cultured with KYSE410 cells at 37°C for 24 h and fixed with 4% formalin, and the nuclei were stained with DAPI; then, the exomes were observed under a fluorescence microscope (Olympus, Tokyo, Japan).

Cell Co-culture Modeling

The synthesized siRNA-NC, AFAP1-AS1-siRNA, mimic-NC, miR-26a mimic, pcDNA-AFAP1-AS1 + mimic-NC, and pcDNA-AFAP1-AS1 + miR-26a mimic (Shanghai GenePharma, Shanghai, China) were transfected into mature M2 macrophages, which were co-cultured with KYSE410 cells 24 h later. Transwell chambers with 0.4- μm aperture were placed in a six-well plate, and 1×10^5 M2 macrophages were seeded into the upper chambers, while 3×10^5 KYSE410 cells were seeded into the lower chambers. Moreover, M2 macrophages without any transfection (oligonucleotides or plasmids) were co-cultured with KYSE410 cells as the M2-exosome group; M2 macrophages that were co-cultured with KYSE410 cells and treated with 5 μM exosome inhibitor GW4896 (HY-19363, MCE, Monmouth Junction, NJ, USA) were used as the M2-exosome + GW4869 group; KYSE410 cells co-cultured with RPMI 1640 medium were used as a control group.

qRT-PCR

Total RNA was extracted with an RNA extraction kit (Invitrogen, Carlsbad, CA, USA). AFAP1-AS1, miR-26a, ATF2, CD68, CD206, U6, and glyceraldehyde-3-phosphate dehydrogenase (GAPDH) primers were designed by Takara (Dalian, China) (Table 1). Then cDNA was obtained by reverse transcription of RNA with the Prime-Script RT Reagent Kit (Takara) based on its instructions (10 μL reverse transcription system). qRT-PCR was performed based on the SYBR Premix Ex Taq II Kit instructions (Takara). The data were analyzed by the $2^{-\Delta\Delta\text{Ct}}$ method to calculate the relative transcription levels of target genes (AFAP1-AS1, miR-26a, ATF2, CD68, CD206, U6, and GAPDH). The experiment was repeated three times, and the final data were averaged.

Western Blot Analysis

Total proteins of cells and exosomes were extracted, and protein concentration was determined using a BCA kit (AmyJet Scientific, Wuhan, Hubei, China). The extracted proteins were mixed with the loading buffer, boiled at 95°C for 10 min, centrifuged, electrophoresed with 10% polyacrylamide gel, and transferred to the membrane,

followed by 1-h blocking with 5% skim milk in Tris-buffered saline with Tween 20 (TBST). Then, ATF2 primary antibody (1:1,000, Cell Signaling Technology, Beverly, MA, USA) was added, along with CD68 primary antibody (1:200, Abcam, Cambridge, MA, USA), CD206 primary antibody (1:200, Santa Cruz Biotechnology, Santa Cruz, CA, USA), CD63 primary antibody (1:200, Santa Cruz Biotechnology), CD81 primary antibody (1:200, Santa Cruz Biotechnology), TSG101 primary antibody (1:1,000, Abcam), GRP49 primary antibody (1:1,000, Abcam), and GAPDH primary antibody (1:1,000, Cell Signaling Technology) for overnight incubation at 4°C. Then, the membranes were developed using enhanced chemiluminescent reagent (Thermo Fisher Scientific). Quantification of signals on western blots was conducted using National Institutes of Health ImageJ imaging and processing analysis software with signaling intensity normalized to GAPDH. The experiment was repeated three times with the data averaged.

Scratch Test

KYSE410 cells (1×10^5) were added to a 24-well plate and scratched with a middle spearhead when they spread over the whole plate. PBS was used to wash off the detached cells and cell debris, and co-cultured KYSE410 cells in each group were seeded into 24-well plates, respectively, followed by the same treatment as described earlier. The cells migrating into the wound were pictured at 0, 24, and 48 h using a microscope (Olympus, Tokyo, Japan). The relative distance between the gaps was captured and measured using an inverted microscope (Olympus).

Invasion and Migration Assay

For the migration assay: serum-free RPMI 1640 medium (100 μ L) was added to the apical Transwell chamber and placed in a 37°C, 5% CO₂ incubator for 1 h to activate the polycarbonate membrane. The trypsin was adopted to detach the co-cultured KYSE410 cells, and the medium was removed by centrifugation at the end of detachment. After PBS washing and centrifugation, the cells were resuspended in serum-free RPMI 1640 medium. After counting separately, the cells were then diluted to 2×10^5 cells/mL, and 100 μ L co-cultured KYSE410 cell suspension in each group was added to the apical chamber, and 600 μ L RPMI 1640 medium containing 20% exosome-free FBS was added to the basolateral chamber for 24-h incubation in a 37°C, 5% CO₂ incubator, followed by 10-min methanol fixation and 10-min 1% crystal violet staining. Eight random fields of view were chosen and photographed under an upright microscope.

For the invasion assay, all steps were the same as for the migration assay described earlier, except that 100 μ L serum-free RPMI 1640 medium was replaced with 100 μ L 50 mg/L Matrigel dilution (1:40) (performed on ice).

Lung Metastasis Experiment

Twenty-four 5- to 6-week-old male BABL/c nude mice (the Center for Animal Experiments of Fujian Medical University, Fujian, China) were divided into 8 groups (3 for each group). Cells in all aforementioned groups were cultured to logarithmic growth phase, detached

and counted, and then made into a cell suspension. Then, the single-cell suspension was adjusted to 5×10^6 cells/mL with serum-free medium, which (100 μ L) was subsequently injected into each nude mouse through the tail vein. All experimental animals in each group were observed and recorded, and 45 days later, the mice were euthanized. The rats' lung tissues, including the trachea and bronchus, were taken out for lung metastasis focus observation, followed by counting the number of lung surface metastases. The lung tissue was fixed in 4% paraformaldehyde solution, dehydrated with gradient ethanol solution, permeabilized with xylene, immersed in wax, embedded in paraffin, and sliced, followed by drying and H&E staining for lung metastasis observation.

RNA FISH

The subcellular localization of lncRNA AFAP1-AS1 in cells was examined by FISH, which was performed based on the instructions of Ribo lncRNA FISH Probe Mix. The coverslip was placed in a 24-well culture plate, and cells were seeded at 6×10^4 cells per well to achieve about 80% cell confluence. After taking out the coverslip, the cells were rinsed with PBS, followed by fixation by 1 mL 4% paraformaldehyde and treatment with proteinase K, glycine, and acetamidine reagent. Then, 250 μ L pre-hybrid solution was added for 1-h incubation at 42°C. Next, the pre-hybrid solution was replaced by 250 μ L lncRNA AFAP1-AS1 hybridization solution (300 ng/mL) with probe for overnight hybridization at 42°C. After 3 PBS/Tween 20 (PBST) washes, DAPI (ab104139, 1:100, Abcam, Shanghai, China) diluted with PBST was added for 5-min nucleus staining in a 24-well culture plate, followed by PBST washing (3 times \times 3 min). Finally, the cells were observed under a fluorescence microscope (Olympus) and photographed after blocked with an anti-fluorescence quencher.

Dual Luciferase Reporter Gene Assay

The binding sites of AFAP1-AS1 and miR-26a were predicted and analyzed at the bioinformatics website (<https://cm.jefferson.edu/rna22/Precomputed/>), and the binding relation was then confirmed by dual luciferase reporter gene assay. The target site sequence (WT) of AFAP1-AS1 and the sequence of site-directed mutagenesis of WT target site (MUT) were synthesized. The pmiR-RB-REPORT vector (Guangzhou RiboBio, Guangzhou, China) was digested with restriction endonuclease, and the synthesized WT and MUT were inserted into the pmiR-RB-REPORT vector (RiboBio) with empty vector simultaneously transfected as a control group. The WT and MUT with correct sequence were used for subsequent transfection. The vectors of MUT and WT were co-transfected with mimic NC and miR-26a mimic, respectively, into KYSE410 cells. After 48 h, the cells were lysed before 5-min centrifugation and supernatant collection. The luciferase assay kit (RG005, Beyotime Institute of Biotechnology, Shanghai, China) was applied to relative light unit (RLU) value determination with firefly luciferase as an internal reference. The ratio of RLU value from Renilla luciferase measurement to that from firefly luciferase detection was the relative fluorescence value. Three repeats were performed in this experiment.

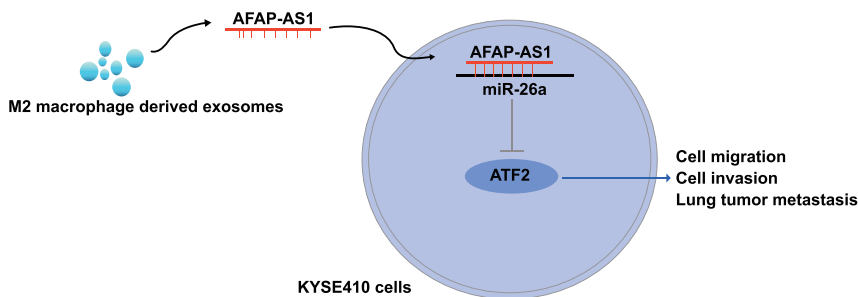


Figure 6. Molecular Mechanism of M2 Macrophage-derived Exosomal lncRNA AFAP1-AS1 in EC

The mechanistic diagram indicates that M2 macrophage-derived exosomes transferred lncRNA AFAP1-AS1 to downregulate miR-26a and upregulate ATF2, thus promoting cell invasion, migration, and lung tumor metastasis of EC.

The targeting relationship of miR-26a and ATF2 and the binding site of miR-26a and the ATF2 3' UTR were predicted with bioinformatics software (<http://www.targetscan.org>). Artificially synthesized segments of ATF2-WT 3' UTR and ATF2 MUT 3' UTR were separately introduced to construct the ATF2 dual-luciferase reporter gene vectors (pmiR-RB-ATF2-3'UTR). The identified ATF2-WT and ATF2-MUT vectors were cotransfected into KYSE410 cells with mimic NC and miR-26a mimic. Cells were lysed, and luciferase activity was detected with a luciferase assay kit. Three repeats were performed in this experiment.

RNA Pull-Down Assay

Biotin-labeled miR-26a oligos (Bio-miR-26a-WT) or mutated oligos (Bio-miR-26a-MUT) or biotinylated NC (Bio-NC) were synthesized by GenePharma (Shanghai, China) and were transfected into KYSE410 cells using Lipofectamine 2000. The final concentration of each biotinylated miRNA was 20 nM. After 48 h, the cell lysates were incubated with M-280 streptavidin magnetic beads (Invitrogen, Waltham, MA, USA) as described previously.³² The bound RNAs were purified using TRIzol; qRT-PCR was used to detect the AFAP1-AS1 levels.

Statistical Analysis

All data were processed with the SPSS v.21.0 software package (IBM, Armonk, NY, USA). The measurement data were expressed as mean \pm standard deviation. The comparison between two groups was made by independent sample t test, and that among multiple groups was made by one-way analysis of variance (ANOVA), after which pairwise comparison was made by Tukey's multiple comparisons test. $p < 0.05$ indicated statistically significant difference.

Conclusions

To sum up, our study indicated that M2-exosomes boosted the invasion and migration of EC cells and that miR-26a overexpression could reverse the contributory impacts of overexpressed AFAP1-AS1 in M2 macrophage-derived exosomes on cell migration and invasion as well as *in vitro* lung tumor metastasis in EC (Figure 6). Also, our work provides novel insights for the role of AFAP1-AS1 in M2-exosomes in EC progression and fresh clues for EC treatment to a certain degree. Nevertheless, further research is still needed for better investigation of the relative mechanism.

AUTHOR CONTRIBUTIONS

X.M. completed the study design. X.M., R.X., and S.H. performed experimental studies. X.M., T.X., W.Z., and M.L. performed data analysis. X.M. completed the manuscript editing. All authors read and approved the final manuscript

CONFLICTS OF INTEREST

The authors declare no competing interests.

ACKNOWLEDGMENTS

We would like to acknowledge the reviewers for their helpful comments on this paper.

REFERENCES

1. Wheeler, J.B., and Reed, C.E. (2012). Epidemiology of esophageal cancer. *Surg. Clin. North Am.* 92, 1077–1087.
2. Zhang, Y. (2013). Epidemiology of esophageal cancer. *World J. Gastroenterol.* 19, 5598–5606.
3. Napier, K.J., Scheerer, M., and Misra, S. (2014). Esophageal cancer: A Review of epidemiology, pathogenesis, staging workup and treatment modalities. *World J. Gastrointest. Oncol.* 6, 112–120.
4. Qian, B.Z., and Pollard, J.W. (2010). Macrophage diversity enhances tumor progression and metastasis. *Cell* 141, 39–51.
5. Jia, Y., Chen, Y., Wang, Q., Jayasinghe, U., Luo, X., Wei, Q., Wang, J., Xiong, H., Chen, C., Xu, B., et al. (2017). Exosome: emerging biomarker in breast cancer. *Oncotarget* 8, 41717–41733.
6. Bastos, N., Ruivo, C.F., da Silva, S., and Melo, S.A. (2018). Exosomes in cancer: Use them or target them? *Semin. Cell Dev. Biol.* 78, 13–21.
7. Min, H., Sun, X., Yang, X., Zhu, H., Liu, J., Wang, Y., Chen, G., and Sun, X. (2018). Exosomes Derived from Irradiated Esophageal Carcinoma-Infiltrating T Cells Promote Metastasis by Inducing the Epithelial-Mesenchymal Transition in Esophageal Cancer Cells. *Pathol. Oncol. Res.* 24, 11–18.
8. Zeng, Z., Bo, H., Gong, Z., Lian, Y., Li, X., Li, X., Zhang, W., Deng, H., Zhou, M., Peng, S., et al. (2016). AFAP1-AS1, a long noncoding RNA upregulated in lung cancer and promotes invasion and metastasis. *Tumour Biol.* 37, 729–737.
9. Wang, F., Ni, H., Sun, F., Li, M., and Chen, L. (2016). Overexpression of lncRNA AFAP1-AS1 correlates with poor prognosis and promotes tumorigenesis in colorectal cancer. *Biomed. Pharmacother.* 81, 152–159.
10. Luo, H.L., Huang, M.D., Guo, J.N., Fan, R.H., Xia, X.T., He, J.D., and Chen, X.F. (2016). AFAP1-AS1 is upregulated and promotes esophageal squamous cell carcinoma cell proliferation and inhibits cell apoptosis. *Cancer Med.* 5, 2879–2885.
11. Yuan, Z., Xiu, C., Song, K., Pei, R., Miao, S., Mao, X., Sun, J., and Jia, S. (2018). Long non-coding RNA AFAP1-AS1/miR-320a/RBPJ axis regulates laryngeal carcinoma cell stemness and chemoresistance. *J. Cell. Mol. Med.* 22, 4253–4262.

12. Jia, L.F., Wei, S.B., Gan, Y.H., Guo, Y., Gong, K., Mitchelson, K., Cheng, J., and Yu, G.Y. (2014). Expression, regulation and roles of miR-26a and MEG3 in tongue squamous cell carcinoma. *Int. J. Cancer* 135, 2282–2293.
13. Li, J., Liang, Y., Lv, H., Meng, H., Xiong, G., Guan, X., Chen, X., Bai, Y., and Wang, K. (2017). miR-26a and miR-26b inhibit esophageal squamous cancer cell proliferation through suppression of c-MYC pathway. *Gene* 625, 1–9.
14. Kumar, A., Bhatia, H.S., de Oliveira, A.C., and Fiebich, B.L. (2015). microRNA-26a modulates inflammatory response induced by toll-like receptor 4 stimulation in microglia. *J. Neurochem.* 135, 1189–1202.
15. Li, Y., Lu, Z., Che, Y., Wang, J., Sun, S., Huang, J., Mao, S., Lei, Y., Chen, Z., and He, J. (2017). Immune signature profiling identified predictive and prognostic factors for esophageal squamous cell carcinoma. *OncoImmunology* 6, e1356147.
16. Arancio, W., Pizzolanti, G., Genovese, S.I., Baiamonte, C., and Giordano, C. (2014). Competing endogenous RNA and interactome bioinformatic analyses on human telomerase. *Rejuvenation Res.* 17, 161–167.
17. Sen, R., Ghosal, S., Das, S., Balti, S., and Chakrabarti, J. (2014). Competing endogenous RNA: the key to posttranscriptional regulation. *ScientificWorldJournal* 2014, 896206.
18. Yin, Z., Ma, T., Huang, B., Lin, L., Zhou, Y., Yan, J., Zou, Y., and Chen, S. (2019). Macrophage-derived exosomal microRNA-501-3p promotes progression of pancreatic ductal adenocarcinoma through the TGFBR3-mediated TGF- β signaling pathway. *J. Exp. Clin. Cancer Res.* 38, 310.
19. Binenbaum, Y., Fridman, E., Yaari, Z., Milman, N., Schroeder, A., Ben David, G., Shlomi, T., and Gil, Z. (2018). Transfer of miRNA in Macrophage-Derived Exosomes Induces Drug Resistance in Pancreatic Adenocarcinoma. *Cancer Res.* 78, 5287–5299.
20. Lau, C., and Henning, S.J. (1989). A noninvasive method for determining patterns of milk intake in the breast-fed infant. *J. Pediatr. Gastroenterol. Nutr.* 9, 481–487.
21. Fu, X.L., Duan, W., Su, C.Y., Mao, F.Y., Lv, Y.P., Teng, Y.S., Yu, P.W., Zhuang, Y., and Zhao, Y.L. (2017). Interleukin 6 induces M2 macrophage differentiation by STAT3 activation that correlates with gastric cancer progression. *Cancer Immunol. Immunother.* 66, 1597–1608.
22. Domper Arnal, M.J., Ferrández Arenas, Á., and Lanás Arbeloa, Á. (2015). Esophageal cancer: Risk factors, screening and endoscopic treatment in Western and Eastern countries. *World J. Gastroenterol.* 21, 7933–7943.
23. Sakai, M., Sohma, M., Miyazaki, T., Yoshida, T., Kumakura, Y., Honjo, H., Hara, K., Ozawa, D., Suzuki, S., Tanaka, N., et al.; Association of Preoperative Nutritional Status with Prognosis in Patients with Esophageal Cancer Undergoing Salvage Esophagectomy (2018). Association of Preoperative Nutritional Status with Prognosis in Patients with Esophageal Cancer Undergoing Salvage Esophagectomy. *Anticancer Res.* 38, 933–938.
24. Arora, H., Qureshi, R., Park, A.K., and Park, W.Y. (2011). Coordinated regulation of ATF2 by miR-26b in γ -irradiated lung cancer cells. *PLoS ONE* 6, e23802.
25. Shen, H., Wang, Y., Shi, W., Sun, G., Hong, L., and Zhang, Y. (2018). LncRNA SNHG5/miR-26a/SOX2 signal axis enhances proliferation of chondrocyte in osteoarthritis. *Acta Biochim. Biophys. Sin. (Shanghai)* 50, 191–198.
26. Tian, S., Yuan, Y., Li, Z., Gao, M., Lu, Y., and Gao, H. (2018). LncRNA UCA1 sponges miR-26a to regulate the migration and proliferation of vascular smooth muscle cells. *Gene* 673, 159–166.
27. Gezer, U., Özgür, E., Cetinkaya, M., Isin, M., and Dalay, N. (2014). Long non-coding RNAs with low expression levels in cells are enriched in secreted exosomes. *Cell Biol. Int.* 38, 1076–1079.
28. Miyata, Y., Fukuhara, A., Otsuki, M., and Shimomura, I. (2013). Expression of activating transcription factor 2 in inflammatory macrophages in obese adipose tissue. *Obesity (Silver Spring)* 21, 731–736.
29. Sahu, S.K., Kumar, M., Chakraborty, S., Banerjee, S.K., Kumar, R., Gupta, P., Jana, K., Gupta, U.D., Ghosh, Z., Kundu, M., and Basu, J. (2017). MicroRNA 26a (miR-26a)/KLF4 and CREB-C/EBP β regulate innate immune signaling, the polarization of macrophages and the trafficking of Mycobacterium tuberculosis to lysosomes during infection. *PLoS Pathog.* 13, e1006410.
30. Ichikawa, T., Sato, F., Terasawa, K., Tsuchiya, S., Toi, M., Tsujimoto, G., and Shimizu, K. (2012). Trastuzumab produces therapeutic actions by upregulating miR-26a and miR-30b in breast cancer cells. *PLoS ONE* 7, e31422.
31. Zhou, X.L., Wang, W.W., Zhu, W.G., Yu, C.H., Tao, G.Z., Wu, Q.Q., Song, Y.Q., Pan, P., and Tong, Y.S. (2016). High expression of long non-coding RNA AFAP1-AS1 predicts chemoradioresistance and poor prognosis in patients with esophageal squamous cell carcinoma treated with definitive chemoradiotherapy. *Mol. Carcinog.* 55, 2095–2105.
32. Subramanian, M., Li, X.L., Hara, T., and Lal, A. (2015). A biochemical approach to identify direct microRNA targets. *Methods Mol. Biol.* 1206, 29–37.